GLOBAL BIOGEOCHEMICAL CYCLES, VOL. 10, NO. 3, PAGES 457–471, SEPTEMBER 1996

Cross–correlation analysis of the dynamics of methane emissions from a boreal peatland

Anu Kettunen[1] and Veijo Kaitala

Systems Analysis Laboratory, Helsinki University of Technology, Espoo, Finland

Jukka Alm and Jouko Silvola

Department of Biology, University of Joensuu, Joensuu, Finland

Hannu Nykänen and Pertti J. Martikainen

Department of Environmental Microbiology, National Public Health Institute, Kuopio, Finland

Abstract. The effects of temperature, water table, and precipitation on the methane fluxes from a boreal low-sedge *Sphagnum papillosum* pine fen were analyzed with statistical cross correlations of daily data. The six measurement sites represented different vegetation surfaces of the mire (hummocks, lawns, and flarks) with increasing moisture. The dynamics were analyzed separately for the early summer (May–July) and the late summer (August–October) periods in addition to the whole summer (May–October) period. Methane emissions increased with increasing peat temperature. During the late summer period, changes in peat temperatures at depths of 20 and 50 cm were reflected in methane emissions within 2 days. The persistently high water tables during the measurement period probably did not reveal the dynamics between water table fluctuations and methane emissions very clearly. Methane emission levels correlated negatively with depths of the water tables, that is, high methane emissions were associated with low water tables and vice versa. The suppression of methane emissions by filling the unsaturated gas space during precipitation and the increased release rate caused by a declining water table could explain the result. Methane emissions correlated positively with changes in water tables, that is, a rise in water table increased methane emissions during the early and whole summer periods. Precipitation increased emissions with a lag from zero to several days throughout the summer. Generally, the estimated responses of methane fluxes to precipitation and changes in water table indicated similar time lags. Methane flux from the flark surfaces seemed to respond rapidly to rainfall and changes in water table with a lag of zero or 1 day. In the lawn–low hummock, the lawn and one hummock site, methane flux showed a slow response with several days lag. This study strongly indicates that temperature, water table, and precipitation affect methane emissions with complex interactions.

Introduction

The high latitude northern (50–70°N) peatlands, most of which belong to the boreal zone, are suggested to contribute 34% of the wetland methane emissions [*Bartlett and Harriss*, 1993]. Annual emissions from wetland ecosystems are estimated to be 110 Tg which corresponds to 20 - 30% of the global methane emissions [*Khalil and Rasmussen*, 1983; *Cicerone and Oremland*, 1988; *Bartlett and Harriss*, 1993;]. Thus, peatlands are a major methane source in the global biogeochemical cycle [*Gorham*, 1991].

Methane is produced in wetlands by methanogenic bacteria as the last step in a chain of anaerobic degradative reactions (for details see *Cicerone and Oremland*, [1988]). Methanotrophic bacteria oxidize methane to carbon dioxide in the opposing reaction [*Cicerone and Oremland*, 1988]. Both the production and oxidation rates as well as the process of transport from peat to the atmosphere affect methane fluxes from peatlands.

[1]Also at Department of Forest Ecology, Helsinki University, Helsinki, Finland.

Paper number 96GB01609.
0886-6236/96/96GB-01609$12.00

Methane is liberated from peat via three routes: diffusion, ebullition, and passage through plants [e.g., *Conrad*, 1989; *Chanton et al.*, 1992].

Methane fluxes from peatlands show high spatial and temporal variations [*Whalen and Reeburgh*, 1988, 1992; *Moore et al.*, 1990; *Morrissey and Livingston*, 1992; *Windsor et al.*, 1992; *Dise*, 1993]. The spatial variation is related to the fact that the basic processes (methane production, oxidation, and transport from peat to atmosphere) are affected by site specific factors such as average hydrological conditions [*Svensson and Rosswall*, 1984; *Sebacher et al.*, 1986; *Bubier et al.*, 1993a, b; *Christensen*, 1993; *Roulet et al.*, 1992, 1993; *Vourlitis et al.*, 1993; *Moore et al.*, 1994], soil nutrient contents [*Svensson and Rosswall*, 1984; *Dise*, 1993], substrate concentration and quality [*Morrissey and Livingston*, 1992; *Whiting and Chanton*, 1992; *Valentine et al.*, 1994; *Schimel*, 1995] and vegetation type [Torn and Chapin, 1993; *Shannon and White*, 1994; *Bubier*, 1995; *Bubier et al.*, 1995; *Schimel*, 1995]. The temporal variation is due to the seasonal cycle of methane emissions with high summer and low winter fluxes [*Dise et al.*, 1993; *Shurpali et al.*, 1993; *Frolking and Crill*, 1994], the interannual variation related to varying weather conditions [*Mattson and Likens*, 1990; *Whalen and Reeburgh*, 1992; *Frolking and Crill*, 1994], the diurnal flux cycle [*Silvola et al.*, 1992; *Mikkelä et al.*, 1995], and episodic high fluxes [*Windsor et al.*, 1992; *Frolking and Crill*, 1994]. However, most studies deal with seasonal averages as data sets are limited both temporally and spatially.

When considering the methane emission dynamics, temperature [*Moore and Knowles*, 1987, 1990; *Crill et al.*, 1988; *Whalen and Reeburgh*, 1988; *Dise et al.*, 1993; *Shurpali et al.*, 1993; *Torn and Chapin*, 1993; *Shannon and White*, 1994] and depth of the water table [*Sebacher et al.*, 1986; *Bubier et al.*, 1993a, b; *Roulet et al.*, 1993; *Shurpali et al.*, 1993; *Funk et al.*, 1994; *Shannon and White*, 1994; *Martikainen et al.*, 1995] have traditionally been cited as the most important factors. Only recently, has the influence of plants on methane emissions been recognized [*Schütz et al.*, 1991; *Chanton and Dacey*, 1991; *Whiting and Chanton*, 1992, 1993; *Bubier*, 1995; *Bubier et al.*, 1995; *Thomas et al.*, 1996]. The control over episodic methane emissions is even less well understood, but it has been suggested that the methane pulses are related to drops in atmospheric pressure and lowering of the water table [*Mattson and Likens*, 1990; *Windsor et al.*, 1992; *Shurpali et al.*, 1993].

As methane is an important radiatively active gas and contributes strongly to the greenhouse phenomenon [*Lashof and Ajuha*, 1990; *Rodhe*, 1990], it is important to understand the response of methane fluxes from wetland ecosystems to global climate change. In particular, there is a need to measure and model the effects of environmental factors on the mechanisms controlling wetland methane dynamics. The interactions between environmental factors and methane emissions are complex, and hence any single environmental factor can hardly be used to predict methane fluxes satisfactorily. Thus modeling of methane emissions requires understanding of the basic processes affecting the methane emissions.

Most methane emission data sets obtained so far are constrained by infrequent measurements, so that analyses are restricted to seasonal averages. Hence it has not been possible to analyze short-term dynamics between environmental variables and methane emissions. In this paper, we present frequent measurements on temperatures, water tables, precipitation, and methane emissions from a boreal low-sedge *Sphagnum papillosum* pine fen. The extensive data set makes it possible to apply cross–correlation analysis in examining the effects of temperature, water table, and precipitation on methane fluxes. On one hand, we analyze the effects of absolute values of temperature, water table, and precipitation on methane emission levels. On the other hand, we study the effects of changes in temperature and water table on methane emissions. Though causal relationships cannot be deduced directly from statistical measures, cross correlations provide information on the possible control mechanisms between the environmental variables and methane emissions and, in particular, the time lags in the system. Autocorrelations, which give information on the rate of change within a single variable, are used in the interpretation of the cross–correlation analysis.

Materials and Methods

Methane Emission Data

The mire complex (Salmisuo, 62°47'N, 30°56'E) is an eccentric bog, split by some minerotrophic strips [*Tolonen*, 1967]. The data presented here were collected at a minerotrophic strip. The methane emissions (CH_4), temperatures (T_0, T_{10}, T_{20}, and T_{50}), water tables (WT), and precipitation (P) were measured in a low-sedge *Sphagnum papillosum* pine fen situated at the margin area of the mire complex. The data were collected during summer 1993.

Gas fluxes from six different collars (Tables 1a and 1b), situated within a few tens of meters apart from each other, were measured. Permanent 60 by 60 cm collars were driven into the peat in the spring, and an automatic flux chamber system was used to record methane emissions once every 5 to 6 hours. Air was circulated from the chambers to a Shimadzu GC-14-A gas chromatograph equipped with a FI detector. The chambers (height 20 cm), installed on the collars for a 20-min measurement period, were operated pneumatically by means of a control program running on a PC, and methane fluxes were calculated from the linear increase of headspace methane concentration during the incubation (for details see *Silvola et al.* [1992]). The depth of the water table was measured immediately before the methane flux at each microsite. Together with the methane emission measurement, the chamber temperature was recorded. The corresponding peat temperature

Table 1a. Vegetation in the Microsites

Microsite	Bottom Layer	Field Layer
Flark A	*S. angustifolium* (100%)	*C. rostrata* (10%), *Er. vaginatum* (10%) and *Er. angustifolium* (5%)
Flark B	*S. angustifolium* (60%) and *S. majus* (40%)	*Sc. palustris* (2%), *C. limosa* (0.5%) and *C. rostrata* (0.1%)
Lawn A	*S. angustifolium* (85%), *S. magellanicum* (10%), *S. russowii* (5%) and *S. papillosum* (0.1%)	*Er. vaginatum* (12.5%), *V. microcarpum* (0.5%), *A. polifolia* (0.5%), *R. chamaemorus* (0.1%) and *Carex pauciflora* (0.1%)
Lawn–low hummock B	Low *S. fuscum* (70%) hummock with *S. angustifolium* (10%) and S. russowii (10%)	*A. polifolia* (10%) and *R. chamaemorus* (7.5%)
Hummock A	*S. fuscum* (85%) hummock with *S. angustifolium* (10%) and *P. strictum* (5%)	*A. polifolia* (10%) and *R. chamaemorus* (10%)
Hummock B	*S. fuscum* (90%) hummock with *S. magellanicum* (7.5%) and *S. angustifolium* (2.5%)	*Em. nigrum* (12.5%), *Ch. calyculata* (1%) and *Er. angustifolium* (1%)

Dominant species in the bottom and field layers and coverage percentages (in parentheses) in the microsites are shown. In the bottom layer, *S.* is *Sphagnum* and *P.* is *Polytrichum*; in the field layer, *A.* is *Andromeda*, *C.* is *Carex*, *Ch.* is *Chamaedaphne*, *Em.* is *Empetrum*, *Er.* is *Eriophorum*, *R.* is *Rubus*, *Sc.* is *Scheuzcheria*, and *V.* is *Vaccinium*.

profile at different (0–2, 10, 20, and 50 cm) depths was measured at one additional selected site close to the collars. The frequent and extensive manual temperature measurements from a number of different sites representing both hummock, lawn, and flark surfaces from the same mire during the same summer of 1993 showed no statistically significant differences in the temperature at a depth of 30 cm among the different microsites (S. Saarnio, University of Joensuu, personal communication, 1996). All data used in this analysis were converted to equally spaced time series using daily averages of the measurements.

The temperature measurements covered the period from early May to the middle of October. Peat surface temperature ranged from -8 to +28°C. The variations in the peat surface temperature are reflected in the peat

Table 1b. Water tables and Methane Emissions From the Microsites

	Water table, cm		mg CH_4 $m^{-2}d^{-1}$	
Microsite	May–July	August–October	May–July	August–October
Flark A	-1.5 (-4.0 – +2.0)		193.4 (22.7-382.8)	
Flark B	-3.1 (-8.0 – +2.0)	-2.5 (-4.8 – +1.0)	159.7 (23.5–393.8)	198.0 (48.9–550.2)
Lawn A	-4.6 (-8.0 – +2.0)		268.5 (37.1-655.7)	
Lawn–low hummock B	-7.6 (-12.0 – -3.0)	-7.3 (-10.0 – -5.0)	145.9 (21.6–344.0)	205.0 (58.0–403.6)
Hummock A	-28.0(-33.0 – -22.0)		86.8 (16.3-270.2)	
Hummock B			53.0 (8.9-130.5)	66.5 (6.2-200.5)

Average water tables (minima and maxima in parentheses) and average methane emissions (minima and maxima in parentheses) from the microsites are shown. Negative values are used for water tables below the peat surface. The water table measurements for hummock B were unreliable and are not shown. For flark A, lawn A, and hummock A data were available till the end of July.

profile with decreasing amplitude toward the deep layers. The peat temperatures at depths of 20 and 50 cm ranged from +3 to +14°C and from 0 to +11°C, respectively. The peat temperatures showed a typical pattern with higher temperatures in the middle of summer (see Figure 1a). Precipitation data were available from the beginning of June to the middle of October. Precipitation ranged from 0 to 30 mm per day (Figure 1b).

The six microsites for measurements of water tables and methane emissions were selected to represent different vegetation surfaces with increasing moisture of the mire (hummocks, lawns and flarks) (Tables 1a and 1b). The average daily methane emissions and depths of the water tables of the microsites are shown in Figures 2a–2f and Table 1b. Note that negative values were ascribed to water tables below the peat surface. For three microsites (flark B, lawn–low hummock B and hummock B, see Tables 1a and 1b and Figures 2b, 2d, and 2f) virgin data covered the period from the beginning of May to the middle of October. In the remaining three microsites (flark A, lawn A and hummock A, see Tables 1a and 1b and Figures 2a, 2c, and 2e) depth of the water table and other factors were manipulated during the August–October period. Thus the August–October data from these microsites did not represent virgin conditions. For this reason, data from early May to the end of July were used in the analysis for flark A (Figure 2a), lawn A (Figure 2c), and hummock A (Figure 2e). To achieve comparability among the microsites, the cross correlations for the May–July period were calculated also for the remaining three microsites (flark B, lawn–low hummock B, and hummock B). For these three microsites that had data for the May–October period, the dynamics of methane emissions were analyzed also for the May–October and August–October periods in addition to the May–July period. The analyses of the May–July and the August–October periods may give information on the differences in the controls of methane emissions during the early and the late summer months. However, the division into the May–July and the August–October periods is arbitrary, as it is connected with the start of the manipulations.

The water table was persistently close to the *Sphagnum* surface and even exceeded the surface in flarks A and B that represented different flark (minerotrophic hollow) surfaces (Figures 2a–2b and Tables 1a and 1b). At flark A, the abundance of *Carex rostrata* indicated conditions with less standing water than those prevailing at flark B (Table 1a). One collar was installed on a *Sphagnum* lawn surface (Figure 2c and Table 1a) referred to as lawn A. The microsite referred to as lawn–low hummock B was mostly lawn surface but contained a low hummock with typical hummock vegetation (Figure 2d and Table 1a). The methane emissions from lawn A and lawn–low hummock B showed a strong seasonal pattern (Figures 2c–2d). Still, the lack of natural data for lawn A in the August–October period made the interpretation of the seasonal pattern difficult. Two collars were located on high hummocks with low water tables, referred to as hummock A and hummock B (Figures 2e–2f and Tables 1a and 1b). Hummock B was situated at the mire edge. The water table measurements from hummock B were found to be unreliable and were not used in the analyses. The methane emissions from hummocks A and B remained relatively low throughout the summer (Table 1b and Figures 2e–f).

As the methane emissions from the microsites are considered (Figures 2a–2f and Table 1b), the intermediately moist lawn A had highest emissions. The emissions from lawn–low hummock B and flarks A and B were in similar range. Hummocks A and B had the lowest emissions.

Autocorrelations and Cross Correlations

Cross-correlation analysis presented in this section is used to analyze the time lags in the daily dynamics of the methane emissions. The autocorrelation function gives insight into the statistical properties of the time series, such as the rate of change within the time series.

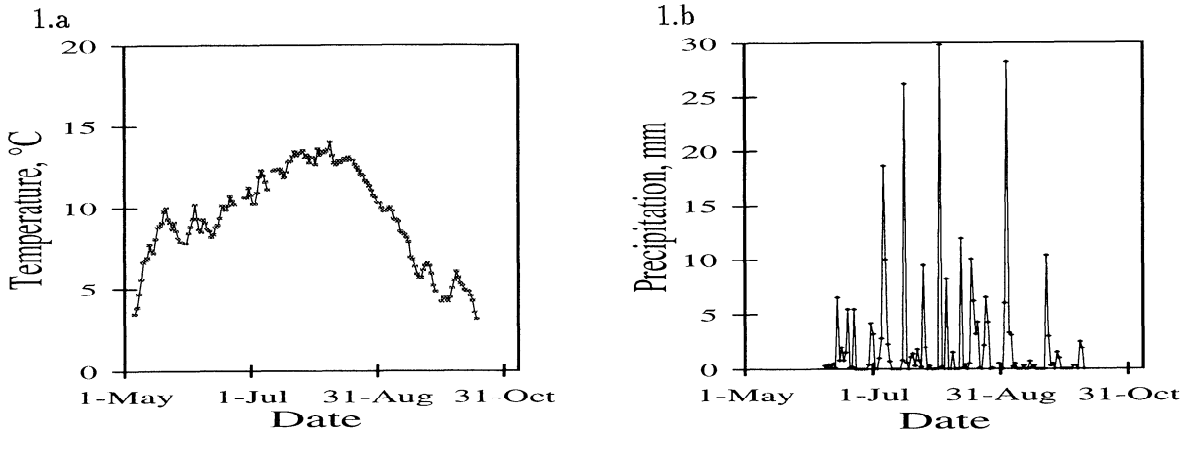

Figure 1. Daily averages of (a) temperature at a depth of 20 cm and (b) precipitation.

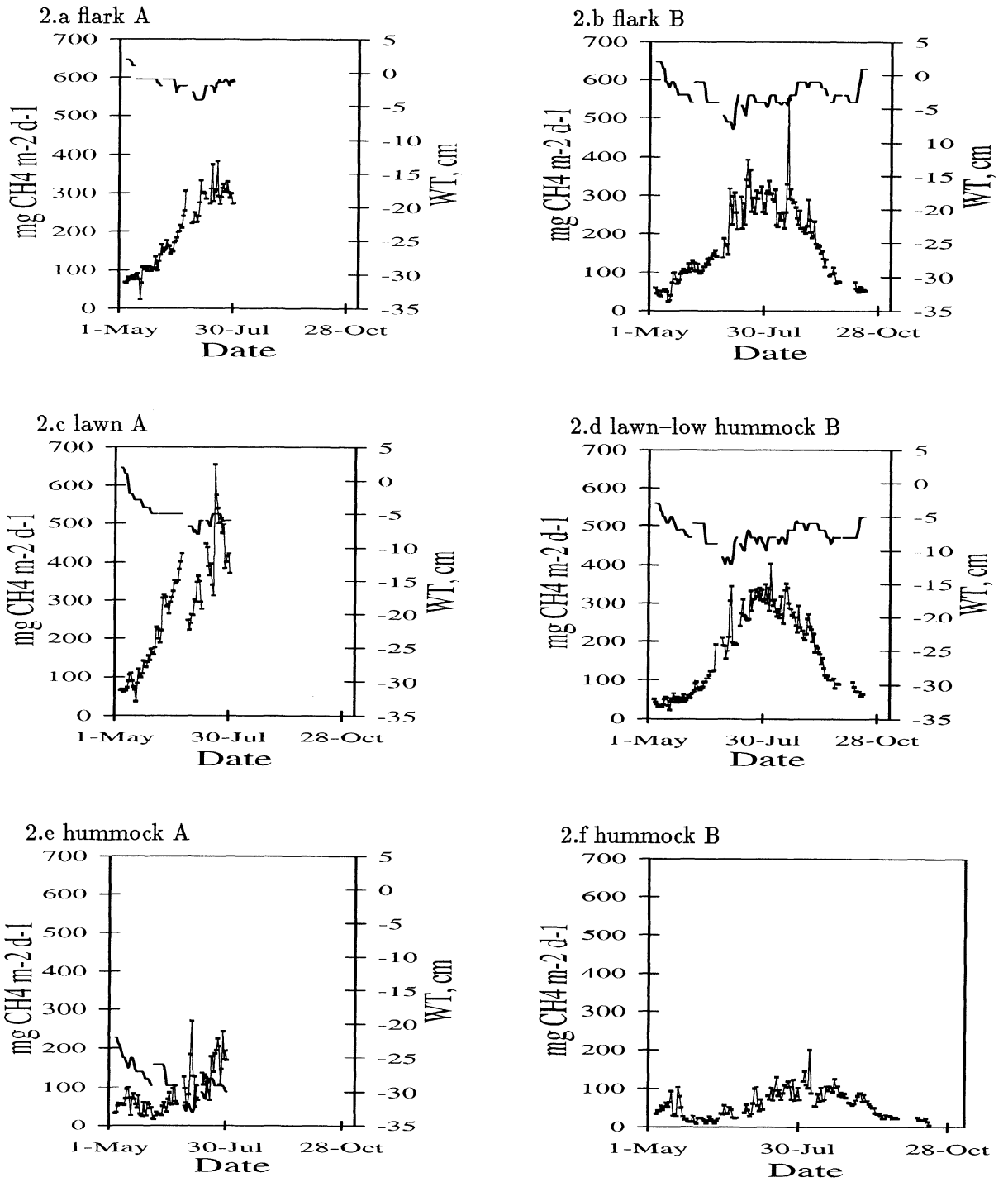

Figure 2. The daily averages of methane emissions (continuous line with squares) and depths of the water table (continuous line) in (a) flark A, (b) flark B, (c) lawn A, (d) lawn–low hummock B, and (e) hummock A, and (f) hummock B. The water table measurements from hummock B were unreliable and are not shown.

Autocorrelations are needed in the interpretation of the cross-correlation functions as autocorrelation peaks affect cross correlations.

The sample estimate for the autocorrelation function of variable x (for example, temperature or precipitation) $\rho_k(x)$ with lag k is technically calculated as

$$\rho_k(x) = \frac{\sum_{n=1}^{N-k}(x_n - \mu_x)(x_{n+k} - \mu_x)}{\sum_{n=1}^{N}(x_n - \mu_x)^2} \quad (1)$$

where N is the number of measurements, k is the lag, and $\mu_x = \frac{1}{N}\sum_{n=1}^{N} x_n$.

The autocorrelation $\rho_k(x)$ lies between -1 and 1 for each k, and $\rho_0(x)$ is equal to 1 by definition. It can be shown that $\rho_k(x)$ is asymptotically normally distributed with mean zero and standard deviation $1/\sqrt{N}$, where N is the number of the observations [see *Pindyck and Rubinfeld*, 1981, p. 500].

Results that hold asymptotically (N approaching infinity) are applied to finite samples with the proviso that the error remains small compared to the effect of choosing a risk level [*Norton*, 1986, p. 49]. Using the ± 95 % confidence intervals of the normal distribution (risk level p=0.05), a sample autocorrelation value $\rho_k(x)$ is significantly different from zero if its absolute value is greater than $2/\sqrt{N}$. In this study, the risk level of 0.05 for autocorrelation was used.

The cross-correlation function can be used to study the time lags of the effect of the control variable x (for example, temperature or water table) on the output variable y (methane emissions). The sample estimate for the lagged cross correlation $r_k(x, y)$ between x and y is calculated as

$$r_k(x,y) = \frac{\sum_{n=1}^{N-k}(x_n - \mu_x)(y_{n+k} - \mu_y)}{\sqrt{\sum_{n=1}^{N}(x_n - \mu_x)^2 \sum_{t=1}^{N}(y_n - \mu_y)^2}} \quad (2)$$

where N is the number of measurements, k is the lag and $\mu_x = \frac{1}{N}\sum_{n=1}^{N} x_n$ and $\mu_y = \frac{1}{N}\sum_{n=1}^{N} y_n$ are the averages for x and y.

The cross-correlation normalization results in values from -1 to 1, the former indicating perfect negative and the latter perfect positive linear relationship. The test statistics used to examine the hypothesis of $r_k(x, y)$ being zero is given by

$$T = \sqrt{N-2}\frac{r_k(x,y)}{\sqrt{1 - r_k(x,y)^2}},$$

which is distributed according to the t distribution with $N-2$ degrees of freedom [*Kleinbaum and Kupper*, 1978, p. 78]. For the cross correlations, a risk level of 0.05 was used for statistical significance, and a risk level of 0.10 was used for weak statistical significance in this study.

The lag k should be small compared to the number N of data points in the time series. When the lag k approaches N, the estimates of the correlation coefficients are based on so few data points that random errors begin to dominate over any real relation between the variables, that is, the noise-to-signal ratio becomes too high. In this study, the maximum lag used is $k = 14$ when the May–October data were available ($N \approx 140$ for flark B, lawn-low hummock B and hummock B) and $k = 7$ when shorter data series from early May to the end of July or from August to October were used ($N \approx 80$ for flark A, lawn A, and hummock A and for flark B, lawn-low hummock B, and hummock B during the May–July or the August–October period).

Unfortunately, some daily values in all time series were missing. When calculating the lagged correlations a data point corresponding to a missing value in the other series (either k days earlier or later) was omitted as well in order to maintain consistency in the temporal difference of the data.

Results

Autocorrelation Functions

The autocorrelation functions of the temperatures at depths of 0–2, 10, 20, and 50 cm (see Figure 3a for a typical temperature autocorrelation) showed strong autoregressive properties, that is $\rho_k(T)$ decreased slowly with increasing k for the May–July, the August–October and the May–October periods. The slow rate of change in the temperatures is related to the seasonal pattern of air temperature, which is slowly reflected in soil temperatures. The slow rate of change which can be deduced from the large ρ_k for $k > 0$ also suggested that temperature dynamics are not easy to identify from measured data.

When the temperature time series were differentiated $\Delta T_i = T_i - T_{i-1}$, the autocorrelation function declined rapidly (see Figure 3b for a typical autocorrelation of the differentiated time series) for all the periods analyzed. The autocorrelations of the differentiated temperatures did not generally differ significantly from zero for lags $k > 1$ (p>0.05 and N=154 for the May–October period). The nonzero autocorrelation coefficients observed in a few cases were probably due to accumulation of random errors in statistically small numbers of data.

The water table time series showed strong autoregressive properties with the autocorrelation function decreasing only slowly with increasing k for the May–October, the May–July, and the August–October periods (see Figure 3c for a typical autocorrelation function of the water table series). Apparently, the slow rate of change in the water table time series makes the system identification difficult with respect to responses to changes in depth of the water table. The slow rate of the change in the water table time series partly related to the extremely low variation in water table position during summer 1993 which makes the interpretation of the cross-correlation analysis even more difficult.

The autocorrelations of the differentiated water table series $\Delta WT_i = WT_i - WT_{i-1}$ declined more rapidly with increasing k than the autocorrelations of WT for the May–July, the May–October, and the August–October periods. Figure 3d shows a typical autocorrelation function of the differentiated water table series. Generally, the autocorrelations of ΔWT for lags $k > 1$ in the five microsites for the different periods did not differ significantly from zero (p>0.05) with some exceptions. For the May–July period, N was 74 for flark A and N was 76 for flark B, lawn A, lawn-low hummock

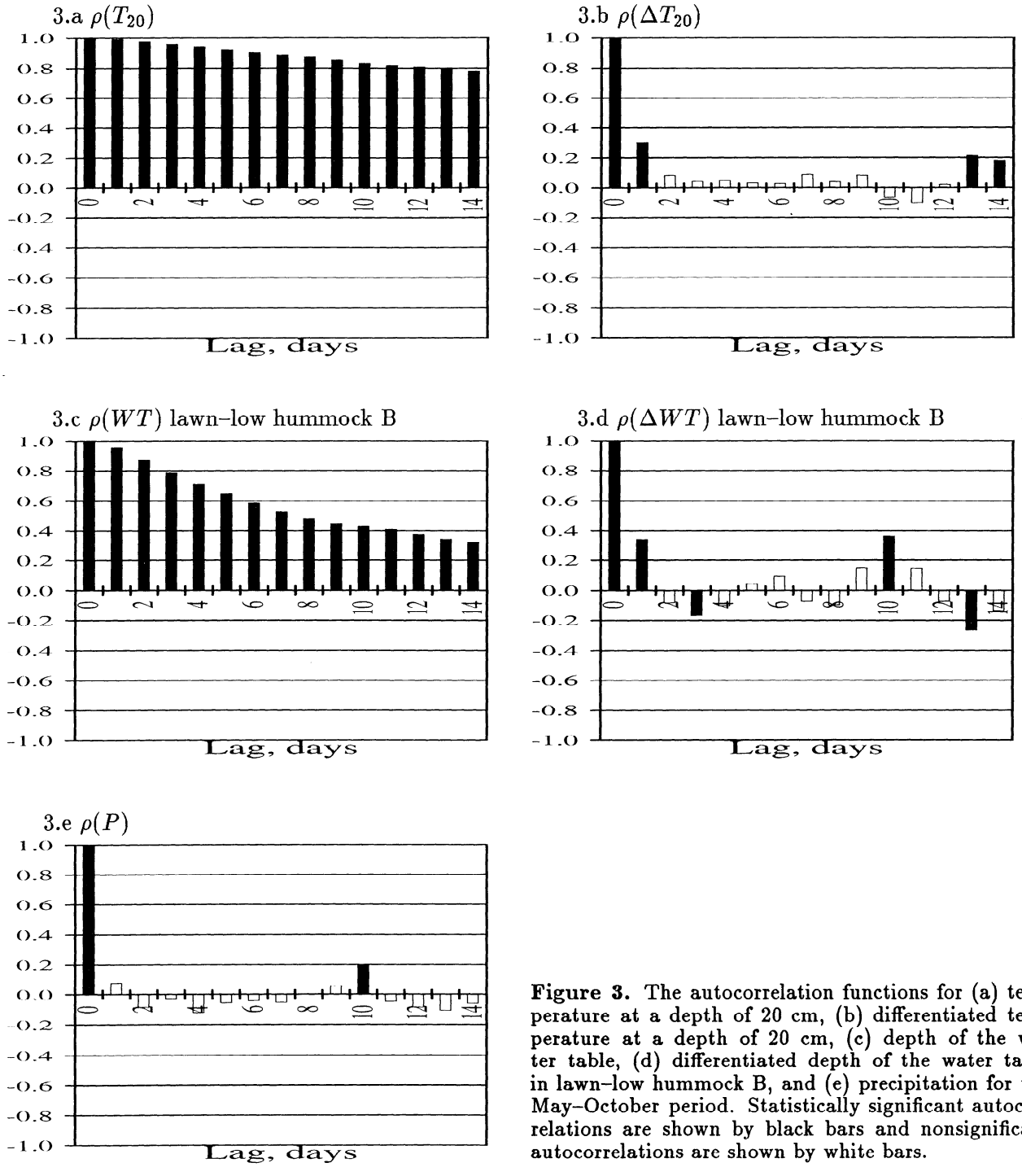

Figure 3. The autocorrelation functions for (a) temperature at a depth of 20 cm, (b) differentiated temperature at a depth of 20 cm, (c) depth of the water table, (d) differentiated depth of the water table in lawn–low hummock B, and (e) precipitation for the May–October period. Statistically significant autocorrelations are shown by black bars and nonsignificant autocorrelations are shown by white bars.

B, and hummock A. N was 72 for flark B and 74 for the lawn–low hummock B during the August–October period. The positive $\rho_9(\Delta WT)$ ($p<0.05$ and $N=149$) for flark B (the autocorrelation not shown) and $\rho_{10}(\Delta WT)$ ($p<0.05$ and $N=150$) for lawn–low hummock B (Figure 3d) might be related to the positive $\rho_{10}(P)$ in the precipitation time series (Figure 3e) during the May–October period via the causal dependence of the water table on precipitation. The negative $\rho_3(\Delta WT)$ and $\rho_{13}(\Delta WT)$ for lawn–low hummock B (Figure 3d) are probably related to the fact that a rise in the water table is followed by a lowering of the water table after a few days. No physical explanation was found to explain the positive $\rho_4(\Delta WT)$ for lawn A (the autocorrelation not shown). These nonzero autocorrelation peaks of ΔWT occur because of accumulation of random errors in the time series.

The autocorrelation of precipitation (Figure 3e) declined rapidly with increasing k, and $\rho_k(P)$ for $k > 0$ stayed near zero. Except $\rho_{10}(P)$, the $\rho_k(P)$ did not

differ significantly from zero (p>0.05 and N=123 for the precipitation time series). Coefficient $\rho_{10}(P)$ statistically differed from zero, but no physical reason was found to explain this. For the May–July and the August–October periods precipitation showed similar autocorrelations as during the May–October period. Unlike temperature and water table, precipitation represented a variable and rich signal which should reveal the dynamics of the system and help in the identification of system interactions.

Temperature Effect on Methane Emissions

The cross–correlation functions between the peat temperatures at different depths and methane emissions indicated that temperature had a strong effect on methane emission (see Figure 4a for a typical cross correlation between temperature and methane emissions). The cross correlations $r_k(T_i, CH_4)$, i=0, 10, 20, and 50 remained above 0.30 for all microsites during the different periods analyzed. The positive correlation for all lags k indicated that at higher temperatures methane emissions were greater. The $r_k(T_i, CH_4)$, i=0, 10, 20, and 50, were clearly statistically significant (p=0.00 and N=81 for flarks A and B, lawn A, lawn–low hummock B, and hummock A and N=80 for hummock B during the May–July period, and N=64 for flark B, N=66 for lawn–low hummock B, and N=63 for hummock B during the August–October period). However, it was not possible to identify whether the actual methane emission was affected by the temperature on the day of measurement or the temperature some days earlier as temperature had strong autoregressive properties.

The cross correlations between the differentiated peat temperatures at depths of 0–2, 10, 20, and 50 cm and methane emissions remained nonsignificant for the May–July period (p>0.05 and N=78 for flark A, lawn A, lawn–low hummock B, and hummock A and N=77

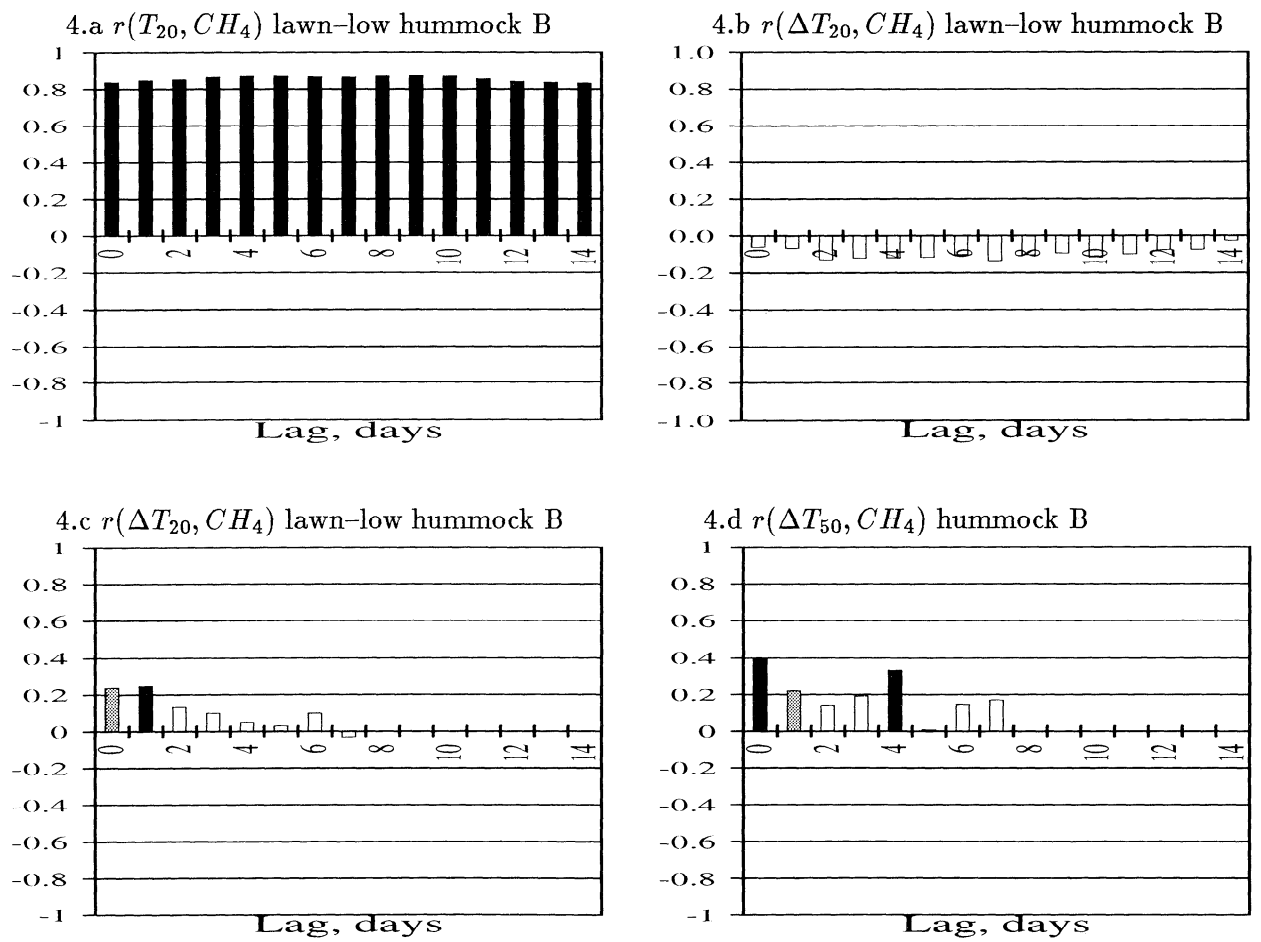

Figure 4. The lagged cross correlation between (a) peat temperature at a depth of 20 cm, (b) differentiated peat temperature at a depth of 20 cm and methane emissions in lawn–low hummock B during the May–October period, (c) differentiated peat temperature at a depth of 20 cm and methane emissions in lawn–low hummock B and (d) differentiated peat temperature at a depth of 50 cm and methane emissions in hummock B during the August–October period. Statistically significant autocorrelations are shown by black bars; weakly significant autocorrelations are shown by gray bars; and nonsignificant autocorrelations are shown by white bars.

for flark B and hummock B, respectively) and for the May–October period (p>0.05 and N=141, 144, and 140 for flark B, the lawn–low hummock B, and hummock B, respectively) (see Figure 4b for a typical cross correlation between the differentiated peat temperature and methane emissions).

For the August–October period, the cross correlations between the differentiated temperature at depths of 0–2 cm and 10 cm and methane emissions were nonsignificant but the cross correlations between the differentiated temperatures at depths of 20 cm and 50 cm and methane emissions indicated that temperatures at deep layers affected methane emissions with a lag of zero to 1 day (Figures 4c–d).

For flark B, $r_1(\Delta T_{20}, CH_4)$ was significant (p<0.02 and N=63) and $r_0(\Delta T_{20}, CH_4)$ was weakly significant (p=0.02 and N=63, the cross correlation not shown). The rises in the temperature at a depth of 50 cm were associated with increased methane emissions from the flark B with a lag of zero to 1 day (p=0.02 for k=0 and p=0.03 for k=1 and N=63, the cross correlation not shown). The cross correlation at lag k=6 was weakly significant (p=0.09 and N=63).

In lawn–low hummock B, significant peaks in the correlation between the differentiated temperature at a depth of 20 cm and methane emissions occurred at lags k=0 and 1 (p=0.05 and p=0.04, respectively, and N=64, Figure 4c). The changes in the temperature at a depth of 50 cm were correlated to methane emissions with lags from zero to 3 days (p=0.05, 0.03, 0.09 and 0.07 for lags k=0, 1, 2, and 3, respectively, and N=64, the cross correlation not shown). In addition, $r_6(\Delta T_{20}, CH_4)$ was weakly significant (p=0.07 and N=64).

For hummock B, the cross correlations were significant at lags k=0 and 1 when the temperature at a depth of 20 cm was considered (p=0.01 and 0.03 and N=66, the cross correlation not shown). In addition, $r_4(\Delta T_{20}, CH_4)$ was weakly significant (p=0.09 and N =66). The significant $r_0(\Delta T_{50}, CH_4)$ (p=0.00 and N =66, Figure 4d) indicated a rise in methane emissions during the same day as the temperature rose. The significant $r_4(\Delta T_{50}, CH_4)$ and weakly significant $r_1(\Delta T_{50}, CH_4)$ (p=0.01 for k=4 and p=0.09 for k=1 and N=66, Figure 4d) again suggested that a rise in temperature is positively reflected to methane emissions.

Water Table Effect on Methane Emissions

Water tables correlated negatively with methane emissions for all six microsites (see Figure 5 for a typical cross correlation between water table and methane emissions). This indicated that the deeper the water table was below the peat surface, the greater the methane emission tended to be. The cross correlations with all lags were statistically significant (p=0.00 and N=79 for flarks A and B and N=80 for lawn A, lawn–low hummock B, and hummock A, respectively, for the May–July period and p=0.00 and N=143 for flark A and N=145 for lawn–low hummock B for the May–October period). For flarks A and B, lawn A, and lawn–low hummock B, the cross correlations between the water tables and methane emissions increased in magnitude with increasing lag k (Figure 5), but for hummock A, the absolute value of the cross correlation decreased with increasing k (the cross correlation not shown). The negative correlations at all lags k are due to the strong autoregressive properties of the water table time series.

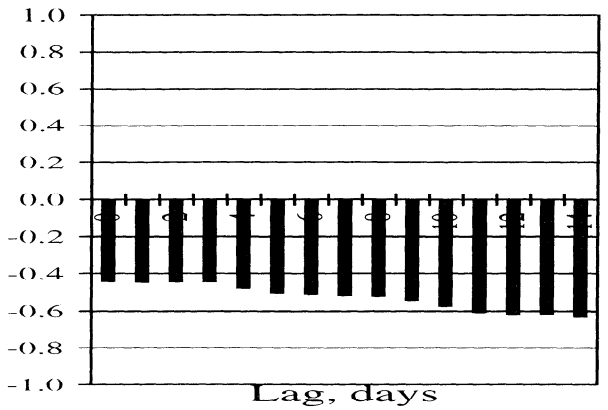

Figure 5. The lagged cross correlation between water tables and methane emissions in lawn–low hummock B for the May–October period. Statistically significant autocorrelations are shown by black bars.

When changes in the depth of the water table (the differentiated water table series) were studied with respect to methane emissions, the cross correlations were positive for all lags in all microsites (Figures 6a–6e). However, the interpretation of the cross correlation peaks was unfortunately not totally straightforward, as the effect of the ΔWT autocorrelation peaks on the cross-correlation function must be carefully considered.

For flark A, no significant (p<0.05 and N=74) peaks were observed (Figure 6a). The cross correlations with lags of k = 1, k = 6, and k = 7 days were weakly significant (p=0.06, 0.07, and 0.08, respectively, and N=74). These peaks were not related to any autocorrelation peaks. The cross correlations with lags k = 6 and k = 7 may be related to the statistically small amount of data, but the $r_1(\Delta WT, CH_4)$ apparently indicated a weak response of increasing methane emissions after a rise in the water table.

For flark B, significant (p<0.05 and N=75) nonzero correlations (the cross correlation not shown) were seen with lags k = 0, k= 2, 5, and 7 in the May–July period. In addition, $r_3(\Delta WT, CH_4)$, $r_4(\Delta WT, CH_4)$, and $r_6(\Delta WT, CH_4)$ were weakly significant (p<0.10 and N=75). The cross correlations for May–October showed a similar response with significant peaks at lags k = 0, k = 8, $\cdots$, 12, and k = 14 (p<0.05 and N=138, Figure 6b). In addition, $r_6(\Delta WT, CH_4)$ was weakly significant (p=0.08 and N=138). The peaks with lag $k > 7$ might be anomalies caused by the strong autocor-

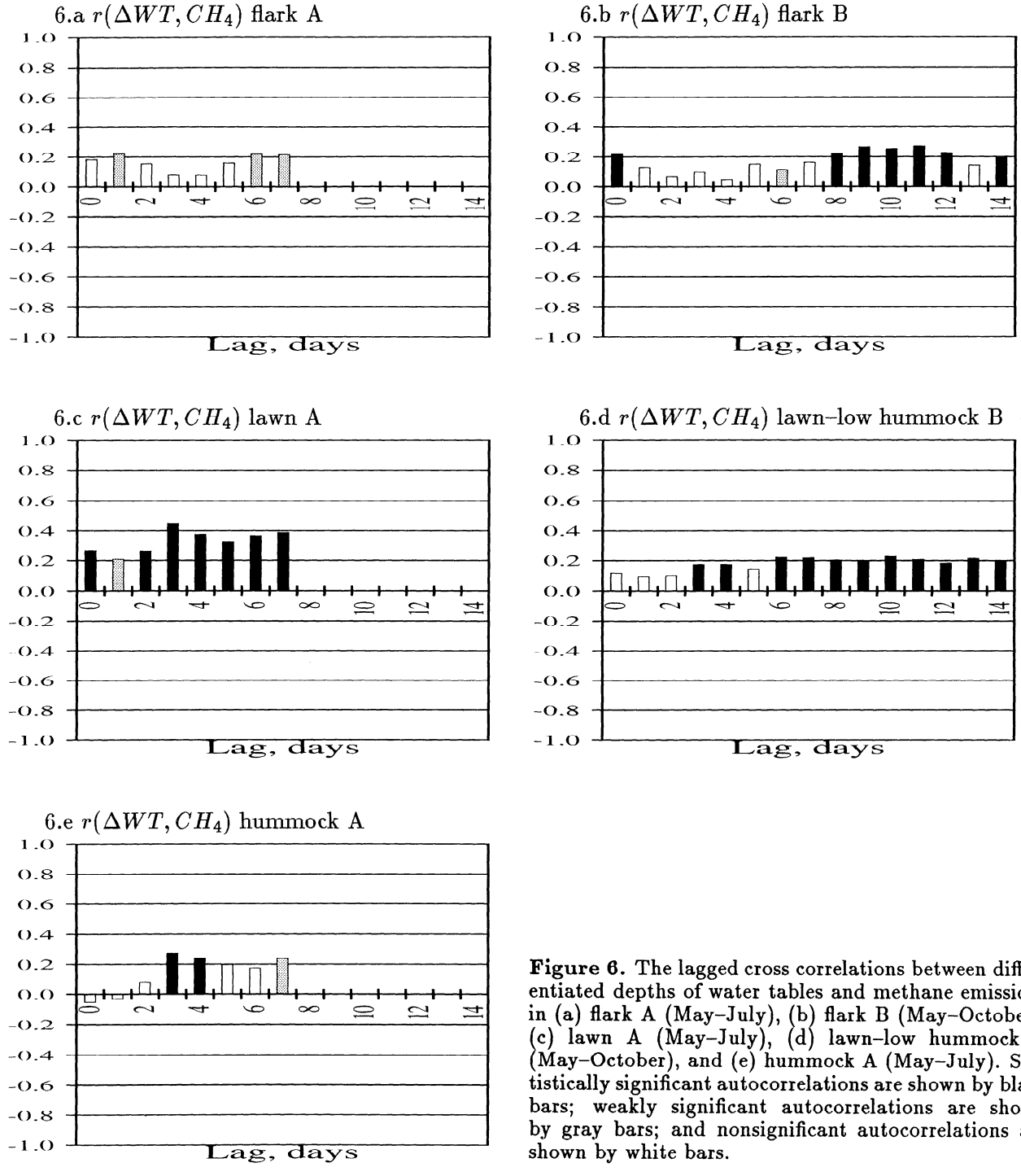

Figure 6. The lagged cross correlations between differentiated depths of water tables and methane emissions in (a) flark A (May–July), (b) flark B (May–October), (c) lawn A (May–July), (d) lawn–low hummock B (May–October), and (e) hummock A (May–July). Statistically significant autocorrelations are shown by black bars; weakly significant autocorrelations are shown by gray bars; and nonsignificant autocorrelations are shown by white bars.

relation $\rho_9(\Delta WT)$, which is probably related to the autocorrelation $\rho_{10}(P)$ (Figure 3e). The $r_0(\Delta WT, CH_4)$ (p=0.01 and N=138), on the other hand, probably showed a real response to a rise in the water table.

The May–July and the May–October period cross correlations suggested that changes in water table are reflected in methane emissions from flark B. However, the August–October period for flark B showed no significant peaks (p>0.10 and N=63, the cross correlation not shown) indicating that changes in the water table play an important role at the beginning of the summer but become less important in the fall.

The cross correlation for lawn A (Figure 6c) was significantly (p<0.05 and N=76) greater than zero for lags $k = 0$ and $k = 2, \cdots, 6$. A weakly significant cross correlation (p=0.07 and N=76) was found at lag $k = 1$. The autocorrelation of ΔWT showed a significant $\rho_4(\Delta WT)$ peak (the autocorrelation not shown), which might be

at least partly responsible for the cross correlation peaks for lags $k > 1$. However, the very high $r_3(\Delta WT, CH_4)$ (p=0.00 and N=76) could not be explained as simply a data anomaly. In addition, the $r_0(\Delta WT, CH_4)$ (p=0.02 and N=76) probably reflected a true rise in methane emissions with rising water table.

As to the water table dynamics in lawn–low hummock B, the cross correlations for the May–July period were significant (p<0.05 and N=76) for lags k = 3, 4, and 6 (the cross correlation not shown) and the cross correlations for the May–October period were significant (p<0.05, N=140, Figure 6d) for lags k = 3 and 4 and $k = 6, \cdots, 14$. The negative autocorrelations of the ΔWT time series at lags k = 3 and k = 13 (Figure 3d) could not cause any of the significant cross correlations. The cross correlations with long lags ($k > 9$) might be anomalies caused by the limited data and the positive autocorrelation $\rho_{10}(\Delta WT)$ (Figure 3d). However, the significant cross correlations with lags k = 3, 4, 6, and 7 (p=0.03, 0.04, 0.04, and 0.01, respectively, and N=76 for the May–July period and p=0.04, 0.04, 0.01, and 0.01, respectively, and N=140 for the May–October period) indicate that the rise in water table was reflected in methane emissions as an increase with a lag of several days.

The May–July and the May–October period cross correlations suggested that changes in the water table are slowly reflected in methane emissions in lawn–low hummock B. However, the August–October period for lawn–low hummock B showed no significant peaks (p>0.10 and N=64, the cross correlation not shown) suggesting that changes in the water table become less important with respect to methane emissions as the summer turns to fall.

For hummock A, significant cross correlations (Figure 6e) occurred with lags k = 3 and k = 4 (p<0.05 and N=76). A weakly significant cross correlation (p=0.05, N=76) was observed with lag k = 7. In this case, the autocorrelation peaks of ΔWT in hummock A could not explain the rise in methane emission, as the significant $\rho_3(\Delta WT)$ and $\rho_4(\Delta WT)$ autocorrelations were negative (the autocorrelation not shown). Thus a rise in the water table was followed by increased methane emissions with a lag of 3 to 4 days.

Precipitation Effect on Methane Emissions

The interpretation of cross correlation between precipitation and methane fluxes was quite straightforward as precipitation was a rich random series with no autoregressive properties. Figures 7a–7f indicated that some days after a rainfall high methane emissions occurred. For flarks A and B, lawn–low hummock B and hummock B the cross correlations were positive with all lags (Figures 7a, 7b, 7d, and 7f). The lawn A and hummock A showed a negative tendency with lags k = 0, 1, and 2, suggesting that rain water may have suppressed the emissions during the first days possibly by filling the unsaturated pore space in peat, and only after a few days did the tendency turn positive (Figures 7c and 7e).

Flark A showed no significant (p<0.05 and N = 48) peaks at the risk level p=0.05 (Figure 7a). However, the cross–correlation coefficient at lag k = 2 was weakly significant (p=0.06 and N = 102). Flark B showed a weakly significant peak $r_2(P, CH_4)$ (p=0.07 and N=47, the cross correlation not shown) during the May–July period. On the basis of the August–October and the May–October periods, the dynamics relating methane emissions to precipitation seemed rather fast in the case of flark B for which significant (p=0.04 and N=55 for the August–October period, p=0.01 and N=102 for the May–October period, Figure 7b) peaks occurred at lags of k = 0 and k = 1 days.

The lawn A dynamics seemed slow as the $r_k(P, CH_4)$ for lags of 1 to 2 days remained negative. Positive, significant (p<0.05 and N=48) peaks occurred at lags k = 4 and k = 5 (Figure 7c). Lawn–low hummock B seemed to respond slowly to precipitation pulses (Figures 7d), but no significant (p<0.05 and N = 48 for the May–July period, N=58 for the August–October period, and N=105 for the May–October period) peaks occurred. With lag k = 4, the cross correlation $r_k(P, CH_4)$ for the May–October period was weakly significant (p=0.05 and N=48, Figure 7d). For the August–October period, weakly significant peaks were seen at lags k=0, 1 and 3 (p<0.05 and N=58).

For hummock A, no significant (p<0.05 and N = 48) peaks were found. Qualitatively, the negative cross correlations for lags k=0, 1, and 2 suggested that precipitation weakly suppressed methane emissions for several days (Figure 7e). For lags $k > 2$, the cross correlations were positive, qualitatively indicating a weak enhancement of methane emissions by precipitation after a lag of several days. For hummock B, the cross correlations between precipitation and the methane emissions remained nonsignificant (p>0.10 and N=47) for the May–July period. The August–October period showed significant peaks at lags k=1 and 4 (p=0.00 and N=55), and the May–October period had similar significant peaks at lags k=1, 4, and 11 days (p=0.00, 0.01, and 0.02, respectively, and N = 102, Figure 7f), suggesting that there might be both a fast and a slow mechanism in the response. The cross correlation $r_{11}(P, CH_4)$, however, might be related to the autocorrelation peak $\rho_{10}(P)$.

Discussion

On the basis of the correlation analysis, the daily methane emissions increased with increasing temperatures. The strong positive correlation between peat soil temperature and methane flux was in accordance with several other studies [*Moore and Knowles*, 1987, 1990; *Crill et al.*, 1988; *Whalen and Reeburgh*, 1988; *Dise et al.*, 1993; *Shurpali et al.*, 1993; *Torn and Chapin*, 1993; *Shannon and White*, 1994]. The strong autocorrelation

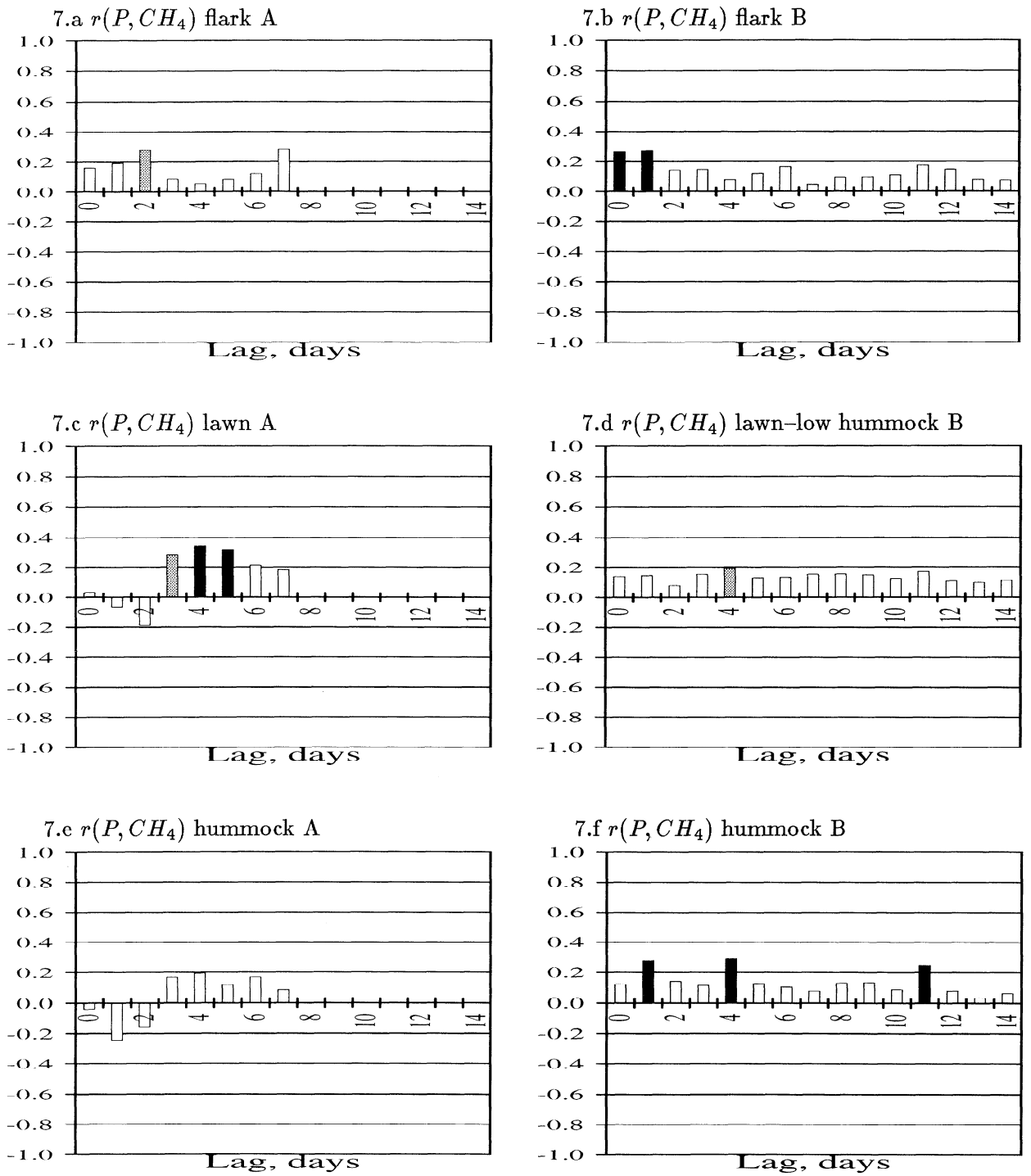

Figure 7. The lagged cross correlation between precipitation and methane emissions in (a) flark A (May–July), (b) flark B (May–October), (c) lawn A (May–July), (d) lawn–low hummock B (May–October), (e) hummock A (May–July), and (f) hummock B (May–October). Statistically significant autocorrelations are shown by black bars; weakly significant autocorrelations are shown by gray bars; and nonsignificant autocorrelations are shown by white bars.

properties of the temperature time series made it difficult to conclude whether temperature affected methane emissions immediately or with a lag.

Methane emissions correlated positively with the differentiated temperatures at depths of 20 and 50 cm for the late summer (August–October). A change in the temperatures at depths of 20 and 50 cm was generally reflected in methane emissions within the first 2 days in these data. For the early summer (May–July) and the whole season (May–October) periods,

methane emissions did not correlate with the differentiated temperature series at any lag. The stronger correlations during the late summer period may indicate the growth of methanogenic population due to better availability of substrates for methanogenesis [*Valentine et al.*, 1994] or merely the effect of temperature on gas transport through vascular plants [*Chanton and Dacey*, 1991; *Thomas et al.*, 1996].

Depth of the water table affects the methane emission with complex interactions. Methane production occurs below the depth of the water table in anaerobic peat, and methane oxidation occurs in aerobic peat [*Sundh et al.* 1994]. Hence, the greater part of the peat profile that was anaerobic, the greater would be the expected flux. In overall terms, the average depth of the water table is actually found to be related to seasonal average methane emission levels [*Sebacher et al.*, 1986; *Bubier et al.*, 1993a, b; *Christensen*, 1993; *Roulet et al.*, 1993; *Moore et al.*, 1994].

The effects of temporal variations in the depth of the water table on methane emissions may, however, be controversial. In this study, methane emissions correlated negatively with depths of the water table for all lags, indicating that high fluxes are associated with lowering water tables. Negative, nonlagged correlations between water tables and methane emissions have been also reported in other studies [*Moore et al.*, 1990; *Whalen and Reeburgh*, 1992]. Lowering of the water table can release pore water methane as laboratory [*Moore and Dalva*, 1993; *Moore and Roulet*, 1993] and in situ measurements [*Moore et al.*, 1990; *Windsor et al.*, 1992; *Shurpali et al.*, 1993] have shown. This causes high fluxes with a drop in the water table. Precipitation has been suggested to suppress the methane emissions [*Frolking and Crill*, 1994], resulting in low emissions with high water tables. However, the water table remained constantly high during the measurement period and thus could only have a limited effect on methane fluxes at individual sites.

When the effects of changes in the water table (the differentiated water table series) were analyzed, methane emissions were found to increase for some days after a rise in the water table and decrease after a fall in the water table for five of the six microsites when data from May–July and May–October periods were studied. During the August–October period, no significant effects of the water table changes on the methane emissions were found.

As suggested by the correlation analysis, precipitation seemed to suppress fluxes, possibly by filling the unsaturated gas space during the first 2 days after rain for two of the six microsites studied (hummock A and lawn A), consistent with results of *Frolking and Crill* [1994]. For the four other microsites, no suppressing effect was seen according to the cross–correlation analysis between precipitation and methane emissions. The results also suggested that precipitation enhanced methane fluxes after a lag of a few days. This finding is consistent with results from studies where lowering of the water table and a drop in atmospheric pressure [*Windsor et al.*, 1992; *Shurpali et al.*, 1993] enhanced methane fluxes.

The estimated responses of methane fluxes to precipitation and to changes in water table generally indicated similar time lags due to the causal dependence of the water table on precipitation. The flarks, which had the highest average water tables, responded fastest (with a lag of zero to 1 day) both to changes in water tables and precipitation. The lawn and the hummock sites, which had low average water tables, showed a slower response with several days' lag with respect to changes in water table and precipitation. The hummock site for which the water table measurements were unreliable responded to rain pulses.

For three of the six microsites, the whole summer season data were available, but for the remaining three, natural data were available only to the end of July. The cross correlations for the different periods were not strictly comparable to each other. The dynamics of methane emissions during the early summer period were found to be different from those during the late summer period. During the May–July period, methane emissions were found to respond to changes in water tables and not to changes in temperatures. Methane emissions were found to be correlated to temperature, but to lack responses to changes in water table during the late summer period. Responses to precipitation remained similar throughout the summer in these data. The differences in the controls for the May–July and August–October period may be related to the availability and quality of substrate [*Valentine et al.*, 1994; *Schimel*, 1995], to the development of vegetation during the summer [*Schütz et al.*, 1991; *Chanton and Dacey*, 1991; *Whiting and Chanton*, 1993; *Schimel*, 1995; *Thomas et al.*, 1996] and to the temporal changes in the microbial populations active in methane production and oxidation [e.g., *Dunfield et al.*, 1993; *Westermann*, 1993].

In this study, the frequent measurements were reduced to a daily basis to analyze the daily dynamics of the methane emissions. A time series of daily data for one summer period is short for statistical analysis, making the interpretation difficult. In addition, the weather during the measurement period was quite atypical, leading to extremely low variation in water tables. Besides, the missing values caused computational difficulties. If the time series were long and stationary, there should be no problem with leaving out some data points in the analysis unless the number of points used in the calculations becomes too small. In this sense, however, the number of points in the present data was quite small. The seasonal pattern of both temperature and methane emissions, in fact, violated the assumption of a stationary series. Furthermore, the correlation among the driving variables within a single season makes it difficult to identify the real emission control mechanisms based on the estimated cross correlations. Analysis of

multiannual measurements would help to tackle with problems related to seasonal pattern and to number of data points. In addition, a great nondomestic data set is still anticipated.

Correlation analysis is a powerful tool for studying the principal interactions in the system, provided that highly nonlinear relationships do not dominate. To date, no other study using lagged cross correlations for identifying the methane emission dynamics is known to the authors. Thus the lagged correlation analysis provides information on the effects of some of the most important environmental factors, temperature, water table, and precipitation, on methane emissions. To conclude, the analyses presented here suggest that changes in temperature and water table and also the occurrence of rain showers are significantly reflected in methane fluxes within a few days. In particular, the analyses show that temporal interactions between environmental variables and methane fluxes are complex, possibly nonlinear dynamic processes.

References

Bartlett, K. B., and R. C. Harriss, Review and assessment of methane emissions from wetlands, *Chemosphere, 26*, 261–320, 1993.

Bubier, J. L., The relationship of vegetation to methane emission and hydrochemical gradients in northern peatlands, *J. Ecol., 83*, 403–420, 1995.

Bubier, J., A. Costello, T. R. Moore, N. T. Roulet, and K. Savage, Microtopography and methane flux in boreal peatlands, northern Ontario, Canada, *Can. J. Bot., 71*, 1056–1063, 1993a.

Bubier, J. L., T. R. Moore, and N. T. Roulet, Methane emissions from wetlands in the midboreal region of northern Ontario, Canada, *Ecology, 74*, 2240–2254, 1993b.

Bubier, J. L., T. R. Moore, and S. Juggins, Predicting methane emission from bryophyte distribution in northern Canadian peatlands, *Ecology, 76*, 677–693, 1995.

Chanton, J. P., and J. W. H. Dacey, Effects of vegetation on methane flux, reservoirs, and carbon isotopic composition, in *Trace Gas Emissions by Plants*, edited T. D. Sharkey, E. A. Holland, and H. A. Mooney, pp. 65–92, Academic, San Diego, Calif., 1991.

Chanton, J. P., C. S. Martens, C. A. Kelley, P. M. Crill, and W. J. Showers, Methane transport mechanisms and isotopic fractionation in emergent macrophytes of an Alaskan tundra lake, *J. Geophys. Res., 97*, 16681–16888, 1992.

Christensen, T. R., Methane emission from Arctic tundra, *Biogeochemistry, 21*, 117–139, 1993.

Cicerone, R. J., and R. S. Oremland, Biogeochemical aspects of atmospheric methane, *Global Biogeochem. Cycles, 2*, 299–327, 1988.

Conrad, R., Control of methane production in terrestrial ecosystems, in *Exchange of Trace Gases Between Terrestrial Ecosystems and the Atmosphere*, edited by M. O. Andreae and D. S. Schimel, pp. 39–58, John Wiley, New York, 1989.

Crill, P. M., K. M. Bartlett, R. C. Harriss, E. Gorham, E. S. Verry, D. L. Sebacher, L. Madzar, and W. Sanner, Methane flux from Minnesota peatlands, *Global Biogeochem. Cycles, 2*, 371–384, 1988.

Dise, N. B., Methane emission from Minnesota peatlands: Spatial and seasonal variability, *Global Biogeochem. Cycles, 7*, 123–142, 1993.

Dise, N. B., E. Gorham, and E. S. Verry, Environmental factors controlling methane emissions from peatlands in northern Minnesota, *J. Geophys. Res., 98*, 10583–10594, 1993.

Dunfield, P., R. Knowles, R. Dumont, and T. R. Moore, Methane production and consumption in temperate and subarctic peat soils: Response to temperature and pH, *Soil Biol. Biochem., 25*, 321–326, 1993.

Frolking, S., and P. Crill, Climate controls on temporal variability of methane flux from a poor fen in southeastern New Hampshire: Measurement and modeling, *Global Biogeochem. Cycles, 8*, 385–397, 1994.

Funk, D. W., E. R. Pullman, K. M. Peterson, P. M. Crill, and W. D. Billings, Influence of water table on carbon dioxide, carbon monoxide, and methane fluxes from taiga bog microcosms, *Global Biogeochem. Cycles, 8*, 271–278, 1994.

Gorham, E., Northern peatlands: Role in the carbon cycle and probable responses to climatic warming, *Ecol. Appl., 1*, 182–195, 1991.

Khalil, M. A. K., and R. A. Rasmussen, Sources, sinks, and seasonal cycles of atmospheric methane, *J. Geophys. Res., 88*, 5131–5144, 1983.

Kleinbaum, D. G., and L. L. Kupper, *Applied Regression Analysis and Other Multivariable Methods*, Duxbury, Boston, Massa., 1978.

Lashof, D. A., and D. R. Ajuha, Relative contributions of greenhouse gas emissions to global warming, *Nature, 344*, 529–531, 1990.

Martikainen, P. J., H. Nykänen, J. Alm, and J. Silvola, Change in fluxes of carbon dioxide, methane and nitrous oxide due to forest drainage of mire sites of different trophy. *Plant Soil, 168-169*, 571–577, 1995.

Mattson, M. D., and G. E. Likens, Air pressure and methane fluxes, *Nature, 347*, 718–719, 1990.

Mikkelä, C., I. Sundh, B. H. Svensson, and M. Nilsson, Diurnal variation in methane emission in relation to the water table, soil temperature, climate and vegetation cover in a Swedish mire, *Biogeochemistry, 28*, 93–114, 1995.

Moore, T. R., and M. Dalva, The influence of temperature and water table position on carbon dioxide and methane emissions from laboratory columns of peatland soils, *J. Soil Sci., 44*, 651–664, 1993.

Moore, T. R., and R. Knowles, Methane and carbon dioxide evolution from subarctic fens, *Can. J. Soil Sci., 67*, 77–81, 1987.

Moore, T. R., and R. Knowles, Methane emissions from fen, bog, and swamp peatlands in Quebec, *Biogeochemistry, 11*, 45–61, 1990.

Moore, T., and N. Roulet, Methane flux: Water table relations in northern wetlands, *Geophys. Res. Lett., 20*, 587–590, 1993.

Moore, T., N. Roulet, and R. Knowles, Spatial and temporal variations of methane flux from subarctic/northern boreal fens, *Global Biogeochem. Cycles, 4*, 29–46, 1990.

Moore, T. R., A. Heyes, and N. T. Roulet, Methane emissions from wetlands, southern Hudson Bay lowland, *J. Geophys. Res., 99*, 1455–1467, 1994.

Morrissey, L. A., and G. P. Livingston, Methane emissions from Alaska arctic tundra: An assessment of local scale variability, *J. Geophys. Res., 97*, 16661–16670, 1992.

Norton, J. P., *An Introduction to Identification*, Academic, San Diego, Calif., 1986.

Pindyck, R. S. and D. L. Rubinfeld, *Econometric Models and*

Economic Forecasts, 2nd ed., McGraw-Hill, New York, 1981.

Rodhe, H., A comparison of the contribution of various gases to the greenhouse effect, *Science, 248*, 1217–1219, 1990.

Roulet, N., R. Ash, and T. Moore, Low boreal wetlands as a source of atmospheric methane, *J. Geophys. Res., 97*, 3739–3749, 1992.

Roulet, N. T., R. Ash, W. Quinton, and T. Moore, Methane flux from drained northern peatlands: Effect of persisting water table lowering on flux, *Global Biogeochem. Cycles, 7*, 749–769, 1993.

Schimel, J. P., Plant transport and methane production as controls on methane flux from arctic wet meadow tundra, *Biogeochemisty, 28*, 183–200, 1995.

Schütz, H., P. Schröder, and H. Rennenberg, Role of plants in regulating the methane flux to the atmosphere, in *Trace Gas Emissions by Plants*, edited by T. D. Sharkey, E. A. Holland, and H. A. Mooney, pp. 29–63, Academic, San Diego, Calif., 1991.

Sebacher, D. I., R. C. Harriss, K. B. Bartlett, S. M. Sebacher, and S. S. Grice, Atmospheric methane sources: Alaskan tundra bogs, an alpine fen, and a subarctic boreal marsh, *Tellus, 38*, 1–10, 1986.

Shannon, R. D., and J. R. White, A three-year study of controls on methane emissions from two Michigan peatlands, *Biogeochemistry, 27*, 35–60, 1994.

Shurpali, N. J., S. B. Verma, R. J. Clement, and D. P. Billesbach, Seasonal distribution of methane flux in a Minnesota peatland measured by Eddy correlation, *J. Geophys. Res., 98*, 20649–20655, 1993.

Silvola, J., P. Martikainen, and H. Nykänen, A mobile automatic gas chromatograph system to measure CO_2, CH_4 and N_2O fluxes from soil in the field, *Suo, 43*, 263–266, 1992.

Sundh, I., M. Nilsson, G. Granberg, and B. H. Svensson, Depth distribution of microbial production and oxidation of methane in northern boreal peatlands, *Microb. Ecol., 27*, 253–265, 1994.

Svensson, B. H., and T. Rosswall, In situ methane production from acid peat in plant communities with different moisture regimes in a subarctic mire, *Oikos, 43*, 341–350, 1984.

Thomas, K. L., J. Benstead, K. L. Davies, and D. Lloyd, Role of wetland plants in the diurnal control of CH_4 and CO_2 fluxes in peat, *Soil Biol. Biochem., 28*, 17–23, 1996.

Tolonen, K., Über die Entwicklung der Moore im finnischen Nordkarelien, *Ann. Bot. Fenn., 123*, 219–416, 1967.

Torn, M. S., and F. S. Chapin III, Environmental and biotic controls over methane flux from Arctic tundra, *Chemosphere, 26*, 357–368, 1993.

Valentine, D. W., E. A. Holland, and D. S. Schimel, Ecosystem and physiological controls over methane production in northern wetlands, *J. Geophys. Res., 99*, 1563–1571, 1994.

Vourlitis, G. L., W. C. Oechel, S. J. Hastings, and M. A. Jenkins, The effect of soil moisture and thaw depth on CH_4 flux from wet coastal tundra ecosystems on the north slope of Alaska, *Chemosphere, 26*, 329–337, 1993.

Westermann, P., Temperature regulation of methanogenesis in wetlands, *Chemosphere, 26*, 321–328, 1993.

Whalen, S. C. and W. S. Reeburgh, A methane flux time series for tundra environments, *Global Biogeochem. Cycles, 2*, 399–409, 1988.

Whalen, S. C., and W. S. Reeburgh, Interannual variations in tundra methane emission: A four year time series at sixed sites, *Global Biogeochem. Cycles, 6*, 139–159, 1992.

Whiting, G. J., and J. P. Chanton, Plant-dependent CH_4 emission in a subarctic Canadian fen, *Global Biogeochem. Cycles, 6*, 225–231, 1992.

Whiting, G. J., and J. P. Chanton, Primary production control of methane emission from wetlands, *Nature, 364*, 794–795, 1993.

Windsor, J., T. R. Moore, and N. T. Roulet, Episodic fluxes of methane from subarctic fens, *Can. J. Soil Sci., 72*, 441–452, 1992.

J. Alm and J. Silvola, Department of Biology, University of Joensuu, P.O. Box 111, FIN-80101 Joensuu, Finland. (e-mail: alm@joyl.joensuu.fi; silvola@joyl.joensuu.fi)

V. Kaitala and A. Kettunen, Systems Analysis Laboratory, Helsinki University of Technology, Otakaari 1 M, FIN-02150 Espoo, Finland. (e-mail: anu.kettunen@hut.fi; veijo.kaitala@hut.fi)

P. J. Martikainen and H. Nykänen, Department of Microbiology, National Public Health Institute, P.O. Box 95, FIN-70701 Kuopio, Finland. (e-mail: pertti.martikainen@ktl.fi; hannu.nykanen@ktl.fi)

(Received January 30, 1996; revised April 16, 1996; accepted May 22, 1996.)